sciendo

172 ENDOCRINE REGULATIONS, Vol. 54, No. 3, 172–182, 2020

doi:10.2478/enr-2020-0020

Cell proliferation and anti-oxidant effects of oxytocin and oxytocin receptors: role of extracellular signal-regulating kinase in astrocyte-like cells

Mohammed M. Alanazi[1,2*], Tomas Havranek[1,3*], Jan Bakos[3,4], Luigi X. Cubeddu[1], Ana M. Castejon[1]

[1]College of Pharmacy, Nova Southeastern University, Fort Lauderdale, Florida, USA; [2]College of Pharmacy, King Saud University, Riyadh, Saudi Arabia; [3]Biomedical Research Center, Institute of Experimental Endocrinology, Slovak Academy of Sciences, Bratislava, Slovakia; [4]Institute of Physiology, Faculty of Medicine, Comenius University, Bratislava, Slovakia

E-mail: castejon@nova.edu

Objectives. Oxytocin (OXT) participates in various physiological functions ranging from reproduction to social and non-social behaviors. Recent studies indicate that OXT affects cell growth and metabolism. Here we characterized the growth stimulating and antioxidant actions of OXT and of OXT receptors (OXTR) in a glial cell-line (U-87MG).

Methods. We developed an OXTR-knockdown cell-line (U-87MG KD) to establish the receptor specificity of OXT's actions, and the impact of lacking OXTR on growth and survival in glial cells. The role Extracellular-Signal Regulated Kinases (ERK1/2) on glial cell protection against consequences of oxidative stress, and cell proliferation was investigated.

Results. In U-87MG cells, OXT stimulated cell proliferation and increased ERK1/2 phosphorylation. The specific ERK1/2 inhibitor, PD098059, produced marked inhibition of cell proliferation, and antagonized the stimulating effect of OXT on ERK1/2 phosphorylation and on cell proliferation. Slower growth rates and lower levels of phosphorylated ERK1/2 were observed in OXTR-knockdown cells and in U-87MG cells treated with an OXTR antagonist (L-371,257). In addition to increasing cell proliferation, OXT significantly blunted the rise in reactive oxygen species induced by H2O2, and antagonized the reductions in cell viability induced by H2O2 and camptothecin. The cell protective and antioxidant actions of OXT in U-87MG cells were not observed in the OXTR-knockdown cells.

Conclusion. OXT stimulates the growth of astrocyte-like cells acting on OXTR via ERK1/2 phosphorylation. The protection against apoptosis and the antioxidant capacity of OXT may contribute to the observed increase in cell proliferation. Oxytocin and OXTR appear to be fundamental for cell growth and viability of glial cells.

Key words: oxytocin, oxytocin receptor, knockdown, proliferation, protection, signaling pathway, hydrogen peroxide, camptothecin

Oxytocin (OXT) is involved in a broad range of physiological processes, ranging from reproduction to social and nonsocial behaviors. In recent years, interest has emerged in the understanding of the effects of OXT on cell growth and cell viability, both in the cardiovascular system and the central nervous system (Cassoni et al. 1998; Bakos et al. 2012). OXT has been shown to induce stimulation of cell growth of endothelial, nerve and glial cells (Cassoni et al. 1998; Cassoni et al. 2006; Bakos et al. 2012; Marinova

Corresponding author: Ana M. Castejon., Ph.D., College of Pharmacy, Nova Southeastern University, 3200 S University Dr., Davie, FL 33328, USA; e-mail: castejon@nova.edu. *The first two authors contributed equally to this work.

et al. 2018) and primary cell cultures of astroglial and hippocampal cells (Palanisamy et al. 2018; Filova et al. 2020). OXT has also been shown to induce mitogenic actions (Ohmichi et al. 1995; Molnar et al. 1999; Szeto et al. 2017), regulated cell cycle, and neurogenesis (Jafarzadeh et al. 2014; Havranek et al. 2017).

The oxytocin receptor (OXTR) is a G-protein-coupled receptor (GPCR) that belongs to the oxytocin/vasopressin subfamily of receptors (Reversi et al. 2005). OXTR was found in the central nervous system and other tissues (Gimpl and Fahrenholz 2001). OXT has demonstrated to have cell-protective and potentially anti-apoptotic actions (Akman et al. 2015). However, evidence that the effects of OXT result from stimulation of OXTR, relies on the use of selective OXTR antagonists (OXTA). Lack of specificity of some of these drugs may induce effects unrelated to OXTR blockade. Experiments on OXTR knockdown cells are needed to better characterize the receptor specificity of OXT's actions and to mimic conditions of OXTR deficiency and absence of receptor-mediated OXT effects.

Extracellular Signal Regulating Kinases 1/2 (ERK1/2) are mitogen activated protein kinase (MAPK) proteins. ERK1/2 proteins are primarily phosphorylated at tyrosine and threonine residues in response to different growth factors. The MAPK cascade plays a role in the cell proliferation, differentiation, survival, and apoptosis (Cha et al. 2012; Sun et al. 2015). Ligands for GPCRs, such as OXT, were found to stimulate the phosphorylation of ERK1/2 (Rimoldi et al. 2003; Devost et al. 2008; Cargnello and Roux 2011; Jurek et al. 2012). For example, OXT induced proliferation of human small cell lung cancer is mediated via activation of ERK1/2 signaling pathway (Pequeux et al. 2004). In the hypothalamic cell line, OXT effect on neurite retraction mediated by MAPK-myocyte enhancer factor 2A pathway has been observed (Meyer et al. 2018). Thus, the MAPK cascade stimulated by OXT is very likely to have functional consequences on neuronal cells.

In this study, we employed a glial U-87MG cell-line and developed an OXTR knockdown cell line (U-87MG KD) to characterize the effects of OXT and OXTR stimulation on glial cells. Oxytocin receptors have been previously found in cultured glial cell lines (Cassoni et al. 1998; Bakos et al. 2012). We investigated the effects of OXT on cell proliferation and determined if OXT exerts protective effects on apoptosis and oxidative stress. In addition, we determined if OXT induced ERK1/2 phosphorylation through OXTR activation is required for OXT's actions on glial cell proliferation.

Oxidative stress, production of reactive oxygen species (ROS) and apoptosis were induced by exposing the various glial types of healthy and tumor cells to hydrogen peroxide (Iida et al. 1997; Lennicke et al. 2015) and camptothecin (CPT) (Djuzenova et al. 2008). Experiments on the OXTR knockdown cell line (U-87MG KD) indicated the growth-stimulating and cell-protective effects of OXT. Noteworthy, OXTR deficiency or blockade resulted in slower cell growth and decreased cell survival.

Materials and methods

Cell culture. Human glioblastoma cell line U-87MG (ATCC HTB-14; ATCC USA, passage 4–14) and related OXTR knockdown cells (passage 5–13) were cultured at a density of ~3×10^5 cells/ml in Dulbecco's modified Eagle's medium (DMEM 1×, 10-013-CV, Corning, USA) with 10% fetal bovine serum (FBS, US origin, 1500-500, VWR Life Science, USA), 1% streptomycin/penicillin (100 µg/ml and 100 Units/ml, respectively, 97063-708, VWR Life Science, USA), and 1% of non-essential amino acids (HyClone, SH30238.01, GE Healthcare Cell Culture, USA). Cells were maintained in a humidified incubator containing 5% of CO_2 at 37 °C. Confluent cells from passages 3 to 10 were used to conduct all proposed experiments. We used 6-well plates to conduct proliferation and Western Blot experiments and 96-well plates for Cell Proliferation Assay (MTT) and ROS experiments. All treatments were done in a full culture medium containing FBS, streptomycin/penicillin and non-essential amino acids. The medium was changed every 24 h, in the presence or absence of different treatments.

Preparation of the U-87MG KD. In order to test our hypothesis, and to prepare *in vitro* condition that mimic linked to OXTR deficiency, we prepared an oxytocin receptor knockdown glioblastoma cell line (U-87MG KD, passage 7). Production of OXTR knockdown cell line followed the previously described technique (see Lestanova et al. 2017). Viral particles were designed by Santa Cruz Biotechnology (Oxytocin-Receptor shRNA Plasmid (h), sc-40154, Santa Cruz Biotechnology, USA). Accession number for the target gene of OXTR is NM 000916. Knockdown control clone and one knockdown OXTR U-87MG clone (U-87MG KD) were successfully selected and established in the culture. U-87MG cells served as controls and were treated the same way except without the silencing shRNA. Stable Knockdown (and knockdown control, respectively) clone cells expressing the shRNA were selected via

puromycin dihydrochloride selection using sufficient amounts of 10 µg/ml in order to eliminate the non-transduced cells as recommended by manufacturer. A reduction of OXTR protein in newly established U-87MG KD clone was verified via Western blot using anti-OXTR antibody (rabbit polyclonal, H-60, 66kDa, sc-33209, Santa Cruz Biotechnology, USA). Based on manufacturer protocol knockdown of oxytocin receptor has been verified (from 85–92%) and stable through several passages (data not shown).

Hemocytometer (cell counting) technique. Cells (U-87MG and U-87MG KD) were cultured overnight at a density of $2x10^4$ cells/ml in full culture medium in 6-well plates. After 48 h stabilization period, cells were incubated in the presence of different concentrations of OXT (H-2510.0005, BACHEM, DE), the OXT antagonist L-371, 257 (OXTA, Santa Cruz Biotechnology, CAS 162042-44-6), or the MEK1/2 inhibitor PD98059 (CST 9900S, Cell Signaling Technology, USA) for 24, 48, 72 and 96 h. The culture medium with treatment was changed every 24 h. At the assigned time points, cells were treated with 300 µl 0.25% trypsin (25-050-Cl, Corning, USA). Once the cells were de-attached, 700 µl of full culture medium was added to each well containing trypsin, and cells were collected into 1.5 ml tubes. A 10 µl aliquot was added to the hemocytometer for cell counting immediately. Results were expressed as number of cells/ml and as percentage of control (untreated) cells.

Flow cytometry. Untreated cells (1×10^5 cells/ml) were cultured in 6-well plates for 8 h. Once the cells were incubated at the assigned conditions, they were then trypsinized and washed with PBS (room temperature, RT). Then, the cells were centrifuged at 1700 rpm for 5 min at 20 °C. The cells were suspended in 400 µl of annexin-V/7-AAD binding buffer (BD Pharmingen™). A 100 µl aliquot (~1×10^5 cells/ml) of the suspended cells was transferred to 1.5 ml tubes and 5 µl of PE annexin V (apoptosis marker) and 5 µl 7-AAD (7-Aminoactinomycin D, necrosis marker) were added to each 1.5 ml tube. Annexin V is commonly used to detect apoptotic cells by its ability to bind to phosphatidylserine, a marker of apoptosis when it is translocated to the cell surface plasma membrane. 7-AAD is commonly used to detect damaged (necrotic) cells as they become non-viable cells in flow cytometry. The cells were then gently mixed and incubated for 15 min at 25 °C in the dark. After incubation, 400 µl of 1x Binding Buffer was added to each 1.5 ml tube and the cells were subsequently analyzed by flow cytometry within 1 h using a BD C6 Accuri Flow Cytometer. The total number of cells was determined, and the percentage of viable cells was calculated by subtracting the annexin V (apoptotic) and 7-AAD (necrotic) positive cells from the total number (~$1x10^5$ cells/ml).

Cell proliferation assay. MTT assay (tetrazolium dye 3-(4,5-dimethylthiazol-2-yl)-2,5-diphenyltetrazolium bromide) is a colorimetric method used to evaluate both cell proliferation and survival based on mitochondrial activity. Cells were cultured, harvested and trypsinized as described above. Further, we have seeded $1x10^4$ cells per well (in 100 µl of full medium) in 96-well plates. The plates were incubated for 24 h. Viability was evaluated in cells incubated in the presence or absence of OXT (100 or 1000 nM) with 750 µM H_2O_2 or 40 µM CPT of oxidative and apoptotic stress inducers for 24 h. For the cell proliferation analysis, the concentration of 750 µM of H_2O_2 was selected due to its optimal effect as an oxidative stressor and the concentration of 40 µM of CPT was selected due to its optimal induction of apoptosis. At the end of the experiment, 50 µl of MTT (1 mg/ml in PBS) reagent was added, kept for 30 min, and followed by addition of 100 µl of DMSO, while shaking for 5 min. Absorbance at 570 nm was recorded by using a micro-plate reader.

Reactive oxygen species assay. We utilized a H2DCFDA kit (Biotium, USA) to quantify ROS levels. It uses the fluorogenic dye 2',7'-dichloroflourescin diacetate (known as DCFDA or H2DCFDA), to measure hydroxyl and other ROS within the cells. Once this dye diffused into the cells, it is deacetylated by the cellular esterase to a non-fluorescent compound, which is subsequently oxidized by the ROS into 2',7'-dichloroflourescin (DCF). DCF is a highly fluorescent compound (excitation 504 nm and emission 529 nm). We have seeded cells (1×10^5 cells/ml) in 6-well plates for 8 h. After this stabilization period, cells were incubated with 500 µM of H_2O_2 for 4 h as middle range effective concentration for this experimental design, in the presence and absence of 100 nM or 1000 nM OXT.

Protein analysis. Proteins were isolated after related experimental time period using lysis buffer (137 mM NaCl, 20 mM Tris-HCl, 10% v/v glycerol) with Pierce Protease Inhibitor cocktail (A32955, Thermo Scientific, USA). Protein concentrations in the samples were established by using the Pierce BCA Protein Assay Kit (23225, Thermo Scientific, USA). In order to adjust the equal amount of loaded proteins, standardize samples dilutions were from 1.0 to 2.0 µg proteins/µl with ultrapure water and Protein Sample Loading Buffer (10% w/v SDS, 0.02% bromophenol blue, and 25% glycerol in 0.5 M Tris-HCl, pH 6.8). For every sample, from 10 µg to 15 µg of isolated protein

were loaded per line for gel separation. Proteins were separated (150 V as constant) by 12% SDS-PAGE separation gels (5% concentration gels, 50 V as constant) by using Mini-Protean Tetra cell system (BioRad, USA). The proteins were transferred (150 V/60 min as constant) to nitrocellulose membrane (BioTrace NT membranes, Pall Corporation, USA) using a Mini Trans-Blot® cell system (BioRad, USA). After blocking (4% w/v Blocking-Grade Blocker in TBS, pH 7.4; BioRad) for 60 min at RT, membranes were incubated overnight at 4 °C with rabbit primary antibodies [anti-ERK1/2 (p44/42 MAPK) rabbit, Cell Signaling Technology, #4695 1:1000 in TBS and anti-phospho-Erk1/2 (p44/42 MAPK), rabbit, Cell Signaling Technology, #9101, 1:1000 in TBS]. After overnight incubation, membranes were incubated with goat anti-rabbit IR-Dye 800CW (925-32211, 1:10 000 in TBS, Li-CoR, USA) secondary antibody for 2 h, at RT. As a reference, the GAPDH protein [anti-GAPDH (D16H11) XP® Rabbit mAb, HPR conjugated, Cell Signaling Technology, #8884S, 1:1000 in TBS] was used without stripping for each membrane. As a Washing solution (3 times for 10 min between each step) TBS-T 0.1% has been used. For signal detection, an Odyssey Fc Infrared Imaging System (LI-COR, USA) was used. The density of each band was quantified and normalized to related GAPDH. Quantification was performed in a single channel; bands of interest were manually shaped with intra-lane (top/bottom) background subtracted using Odyssey Image Studio-Lite 5.2 analytical software (LI-COR, USA).

Statistical analysis. Results are expressed as means ± SEM of a minimum of 4 experiments in triplicates per group. Statistical comparisons were performed via Sigma-Stat 3.1 using Student's t-test and Bonferroni's adjustment for Two-Way ANOVA when needed. The value of $p \leq 0.05$ was considered statistically significant.

Results

Effect of OXT and OXTR knockdown on the cell proliferation and viability. The exposure of U-87MG cells to OXT induced a time- and concentration-dependent increase in cell proliferation (Figure 1A). The significant ($p<0.01$) stimulation of cell proliferation induced by OXT compared to corresponding untreated controls was observed at the highest OXT concentration. The greatest effects were observed at 96 h of exposure to 1 μM OXT (11.1±1.8-fold from baseline vs. the 7.68±0.9-fold from baseline observed

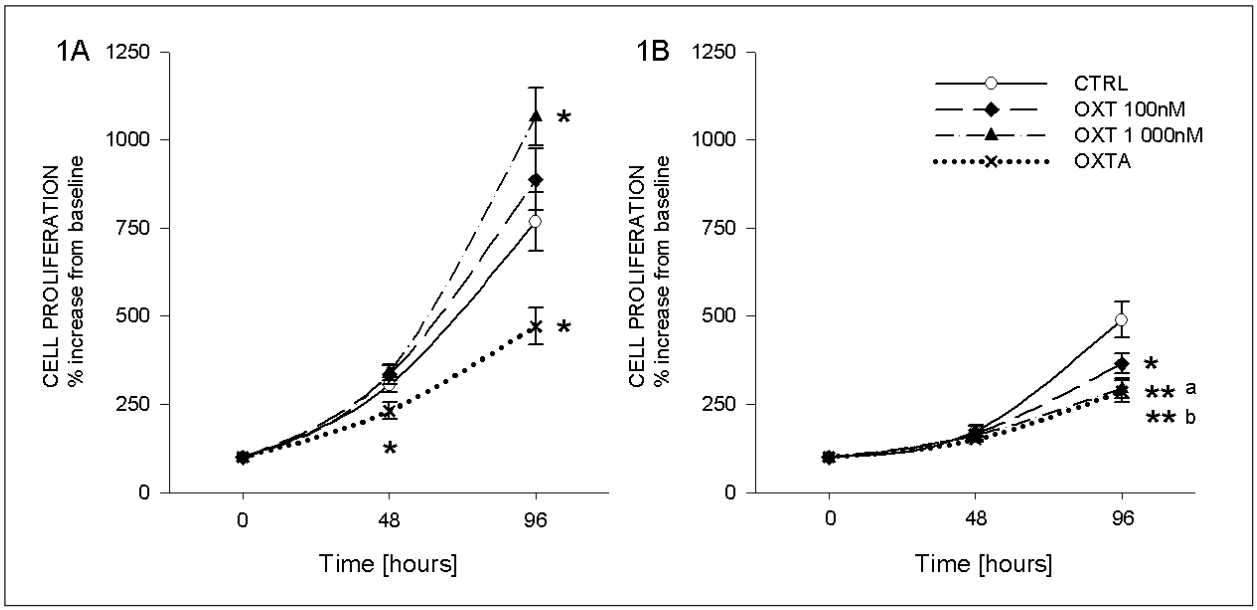

Figure 1. Effects of oxytocin (OXT) on the proliferation of U-87MG **(A)** and U-87MG KD **(B)** cells. Cells were incubated with and without OXT (100 nM and 1000 nM) or 1000 nM oxytocin receptor antagonist (OXTA) for 48, 96 h. Cells were counted with a hemocytomer every 48 h. Results are expressed as the mean percentage increase in the total cell number from baseline values ± SEM (n=4–6). Statistical comparisons were performed employing Bonferroni's adjustment for Two-Way ANOVA. Significantly different values are marked with *$p<0.05$ and **$p<0.01$; **a=$p<0.01$ valid for 96 h treatment with 1000 nM OXT and **b=$p<0.01$ valid for 96 h treatment with 1000 nM OXTA, all compared to untreated controls.

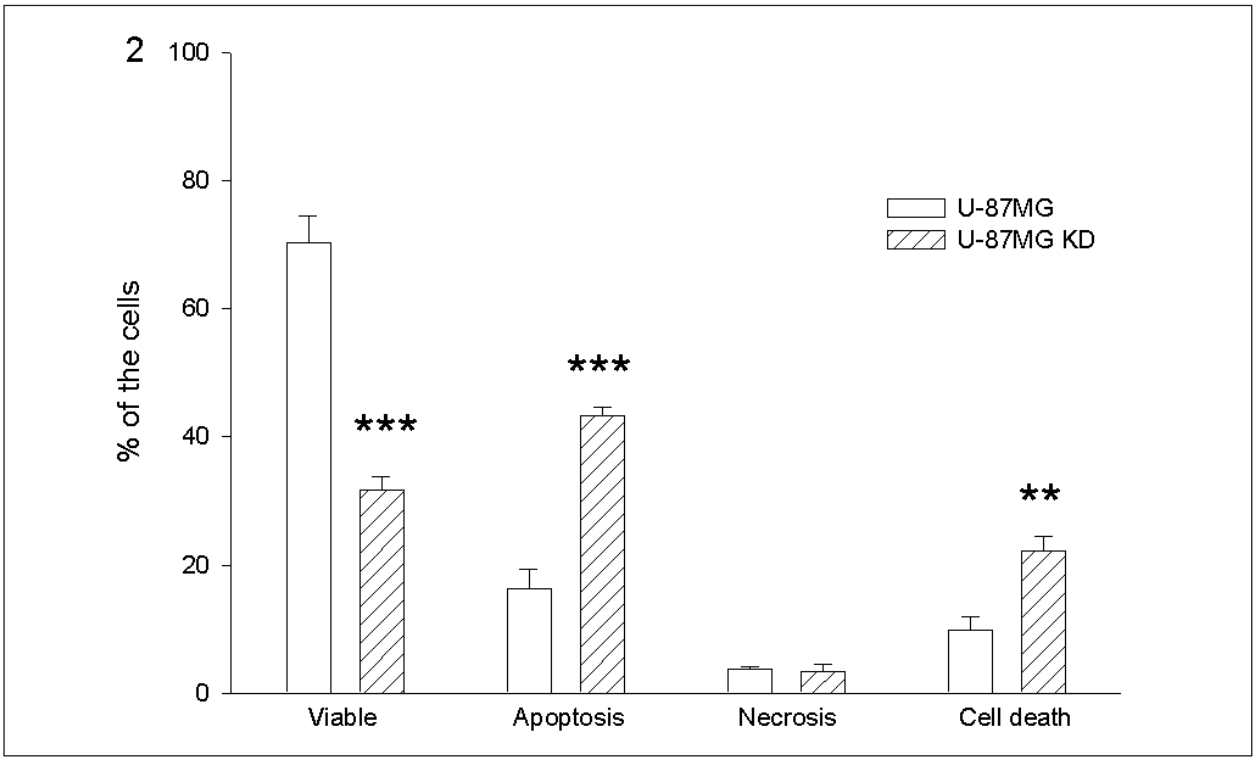

Figure 2. Effects of oxytocin receptor (OXTR) knockdown on cell viability, apoptosis, and cell death. U-87MG and U-87MG KD cells were stained with an apoptosis marker (Annexin V) and a necrosis marker (7-AAD). Viable/non-viable ratio of the cells was analyzed by BD C6 Accuri Flow cytometer (n=4–6). Statistical comparisons were using Student's t-test. Significantly different values are marked **p<0.05 and ***p<0.001.

in control, untreated cells). Exposure to 100 nM OXT for 96 h induced an 8.9-fold marked although non-significant increase from baseline. OXT failed to stimulate cell growth in OXTR knockdown cells and in cells pretreated with OXTR antagonist L-371,257 (Figure 1B). Not only OXT did not stimulate cell proliferation in OXTR knockdown cells, but produced additional inhibition of cell proliferation (100 nM and 1 μM OXT inhibited by 25±5% and 39.6±5%, respectively; p<0.01).

Compared to U-87MG cells, the OXTR knockdown cells showed a slower rate of cell growth (Figure 1B). At 96 h of culture, the number of OXTR knockdown cells increased 4.8 ±0.6-fold from baseline, compared to the 7.68±0.8-fold rise observed for U-87MG cells (p<0.01). Flow cytometry experiments revealed that compared to the U-87MG cells, the OXTR knockdown cells showed significant reductions in the number of viable cells (p<0.001), and a greater percentage of apoptotic, and of necrotic and apoptotic cells (p<0.001) (Figure 2). Similarly, exposure for 96 h to 1 μM L-371,257, an OXTR antagonist, inhibited cell proliferation (38.7±6% inhibition; 4.71±0.7-fold from baseline; p<0.05) (Figure 1B).

OXT stimulated ERK1/2 phosphorylation mediates cell proliferation. OXT induced a time and concentration-dependent increase in ERK1/2 phosphorylation in U-87MG cells (Figure 3A). A 2.2±0.4 and a 3.31±0.8-fold increase in ERK1/2 phosphorylation was observed at min 5 during exposure to 100 nM OXT and 1000 nM OXT, respectively (p<0.01 and p<0.001). OXT-induced increase ERK1/2 phosphorylation was antagonized by L-371,257 and was not observed in OXTR knockdown cells (Figure 3). Treatment with L-371,257 induced a small decrease in ERK1/2 phosphorylation in control U-87MG cells and had no effect on the OXTR knockdown cells (Figures 3C–D).

In order to confirm that the cell proliferative effects of OXT are mediated through activation of the MAPK-ERK1/2 signaling pathway, experiments were conducted in the presence and absence of PD098059, an ERK1/2 inhibitor. PD098059 inhibited cell proliferation, and antagonized the stimulating effect of OXT on cell proliferation (Figure 4). PD098059 significantly inhibited ERK 1/2 phosphorylation and prevented OXT-induced stimulation of ERK1/2 phosphorylation (p<0.001) (Figure 4).

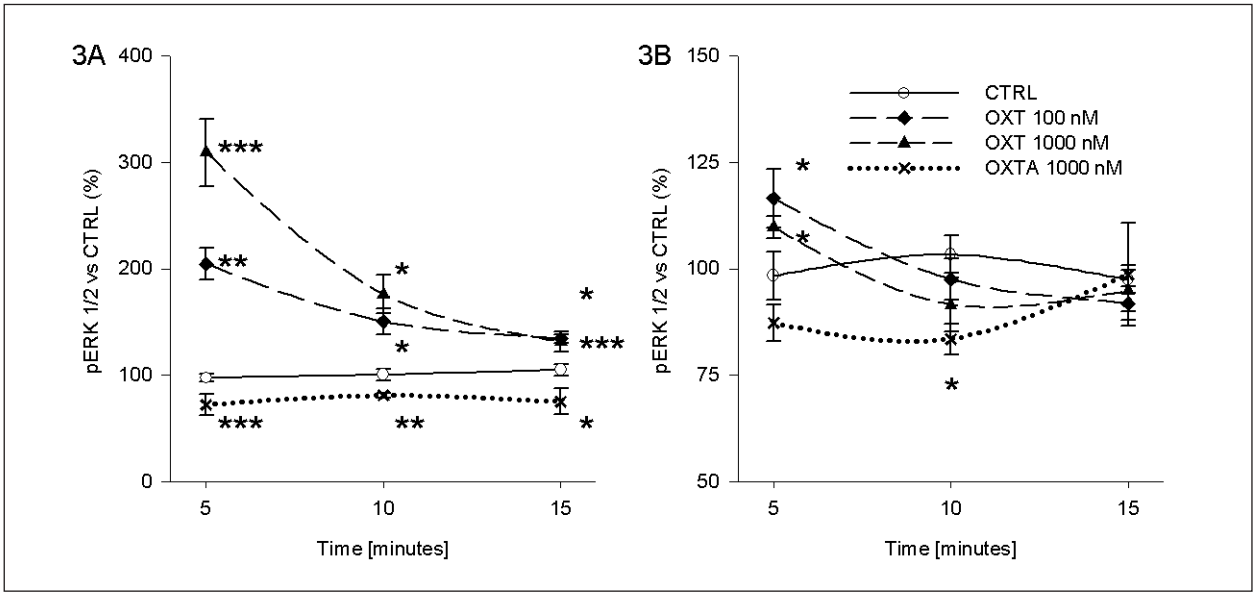

Figure 3. Concentration and time dependent effect of oxytocin (OXT) on ERK1/2 phosphorylation in U-87MG **(A)** and U-87MG KD **(B)** cells. Cells were incubated with and without OXT (100 nM and 1000 nM) or 1000 nM oxytocin receptor antagonist (OXTA) for 5, 10 and 15 min. Level of phosphorylated ERK1/2 (pERK1/2) was determined by Western Blot **(C, D)**. Results are expressed as the mean percentage change in ERK1/2 phosphorylation compared to control values ± SEM (n=4–6). Statistical comparisons were performed employing Bonferroni's adjustment for Two-Way ANOVA. Significantly different values are marked with *p<0.05; **p<0.01 and ***p<0.001.

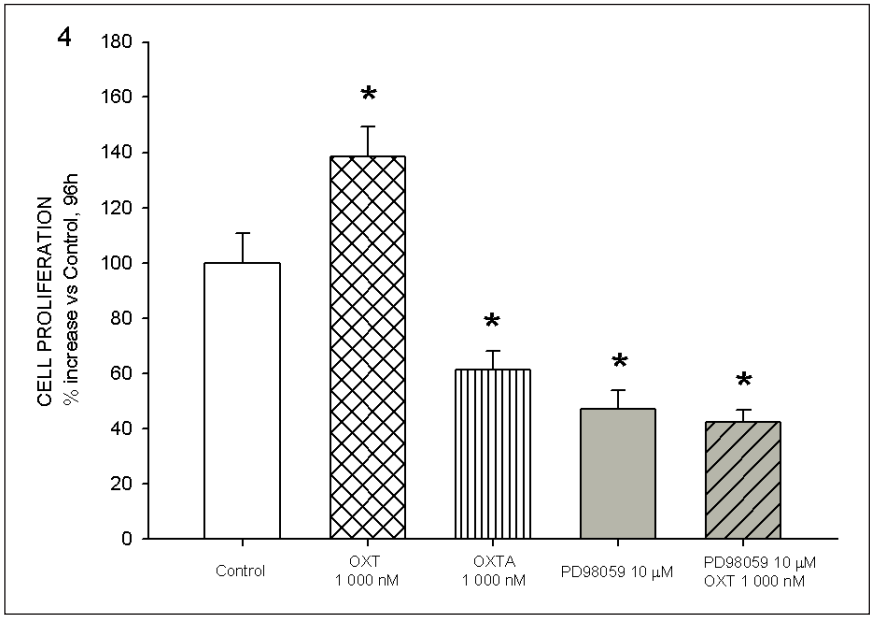

Figure 4. Effects of PD98059 on oxytocin (OXT)-induced increase in cell proliferation. The cells were incubated with and without OXT (100 nM and 1000 nM) or 1000 nM oxytocin receptor antagonist (OXTA) for 96 h. The cells were incubated in a presence of 10 µM PD98059 (selective ERK1/2 inhibitor) for 30 min. Cells were directly counted with a hemocytomer. Results are expressed as the mean percent increase in the total cell number from related untreated control values ± SEM (n=4–6). Statistical comparisons were using Student's t-test. Significantly different values are marked with *p<0.05.

Protective effects of OXT against H_2O_2- and camptothecin-induced cytotoxicity. The exposure of U-87MG cells to H_2O_2 decreased the survival of U-87MG cells. Exposure to 750 µM reduced cell survival by 30.5±3% when compared to the control-untreated group (p<0.001). OXT significantly antagonized the reduction in cell survival induced by 750 µM H_2O_2 (p<0.001). The 30.5±3% decrease in cell viability induced by 750 µM H_2O_2, was reduced to 14.4±3% (p<0.01) and 10.4±3% (p<0.01) by 100 and 1 µM OXT, respectively. L-371,257 abolished the protective effect of OXT on H_2O_2-induced cytotoxicity (Figure 5A).

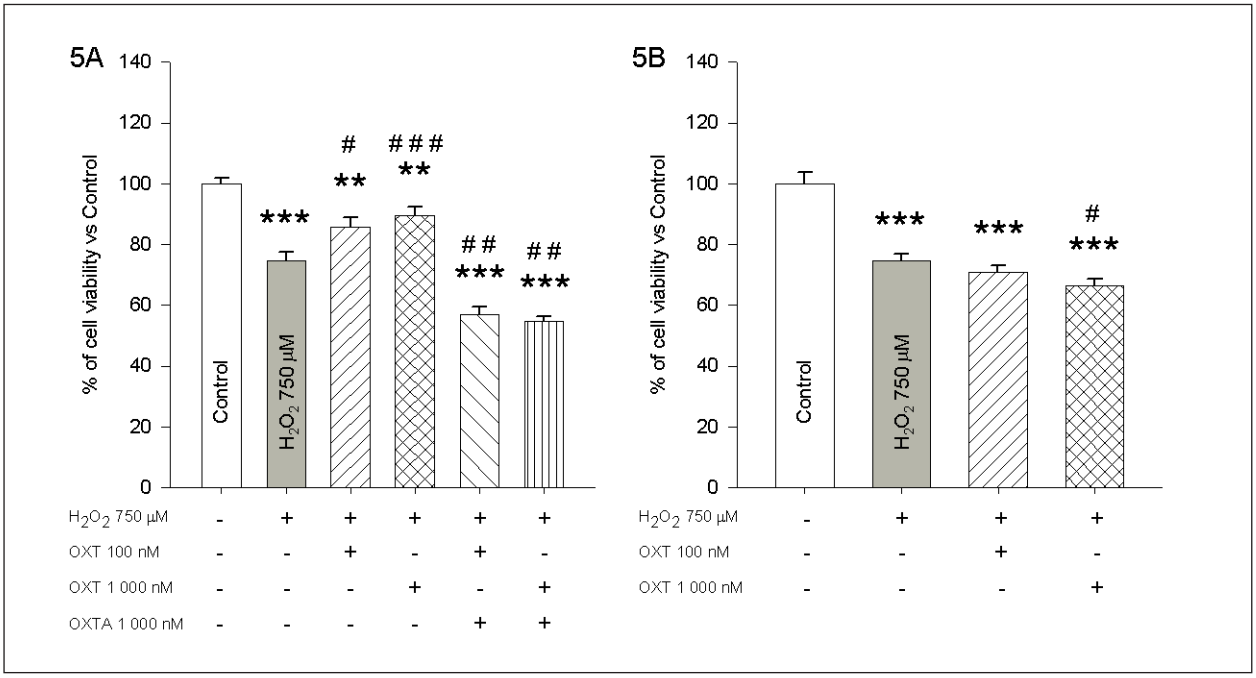

Figure 5. Effects of oxytocin (OXT) on H_2O_2-induced cytotoxicity. U-87MG and U-87MG KD cells were treated for 24 h with 750 µM H_2O_2 in the presence or absence of OXT (100 and 1000 nM) or 1000 nM oxytocin receptor antagonist (OXTA). Results are expressed as the mean percentage change in cell viability ± SEM (n=4–6). Statistical comparisons were performed employing Bonferroni's adjustment for Two-Way ANOVA. Significantly different values are marked with**p<0.01 and ***p<0.001 compared to the control group. $^{\#}$p<0.05, $^{\#\#}$p<0.01 and $^{\#\#\#}$p<0.001 compared to the group treated with H_2O_2 alone.

OXT failed to protect against the H_2O_2 cytotoxicity in the OXTR knockdown cells (Figure 5). In addition, there were no significant differences in the decrease in cell viability induced by 750 µM H_2O_2 in controls and OXTR knockdown cells (29.5±3% vs. 25.4±4%, n.s.).

Exposure of U-87MG cells to camptothecin (CPT; 40 µM) for 24 h decreased cell viability by 31.2±4% (p<0.001). The decrease in cell viability induced by 40 µM CPT was attenuated by 100 and 1 µM OXT from 31.2±4% to 16.7±3% (p<0.001) and 18.4±3% (p<0.001), respectively (Figure 6A). L-371,257 antagonized the protective effect of OXT on CPT-induced cytotoxicity in U-87MG cells (Figure 6A). In OXTR knockdown cells, OXT (100 and 1 µM) failed to prevent CPT-induced cytotoxicity (Figure 6B). Comparable reductions in cell survival were observed in the group treated with CPT alone (30.5±4%) and with CPT+1 µM OXT (30.2±4%) (Figure 6B). Further, comparable reductions in cell viability with CPT were observed in U-87MG and OXTR knockdown cells (Figures 6A, B).

Effect of oxytocin on ROS production induced by H_2O_2. H_2O_2 increased the intracellular production of ROS in U-87MG cells in a concentration-dependent manner. Compared to the control groups, the percent increase in ROS production averaged 18.9±3% with 300 µM (p<0.05), 29.8±4% with 500 µM, and 48.8±5% with 1000 µM H_2O_2 (p<0.01). A middle-range concentration of H_2O_2 (500 µM) was selected for the experimental design involving OXT treatment. OXT inhibited the increase in ROS induced by H_2O_2 (p<0.001) in control U-87MG cells, but exerted no inhibitory effect in the OXTR knockdown cells (Figure 7). There were no significant differences for the increases in intracellular ROS levels induced by H_2O_2 in U-87MG and OXTR knockdown cells (Figure 7).

Discussion

We demonstrated that OXT stimulates the growth of astrocyte-like U-87MG cells and that this effect of OXT was not observed in OXTR knockdown cells and U-87MG cells treated with an OXTR antagonist. Our findings suggest that activation of OXTR by OXT mediates the glial cell growth increase. Cell proliferative effects of OXT have also been described in other endothelial, nerve and glial cell lines (Cassoni et al. 2006; Bakos et al. 2012), and in primary cells, such

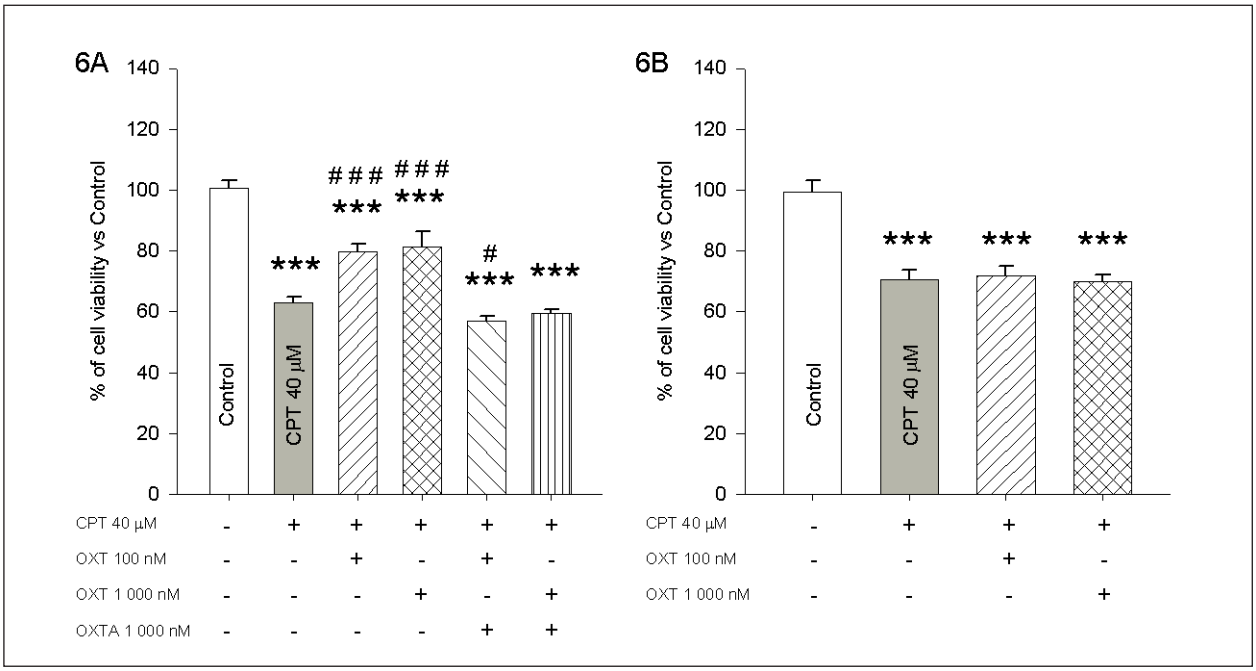

Figure 6. Effects of oxytocin (OXT) on camptothecin (CPT)-induced cytotoxicity. U-87MG and U-87MG KD cell were treated for 24 h with 40 µM CPT in the presence or absence of OXT (100 and 1000 nM) or 1000 nM oxytocin receptor antagonist (OXTA) in the case of U-87MG cells. Results are expressed as the mean percentage change in cell viability ± SEM (n=3–6). Statistical comparisons were performed employing Bonferroni's adjustment for Two-Way ANOVA. Significantly different values are marked with ***p<0.001 compared to the control group. #p<0.05 and ###p<0.001 compared to the group treated with CPT alone.

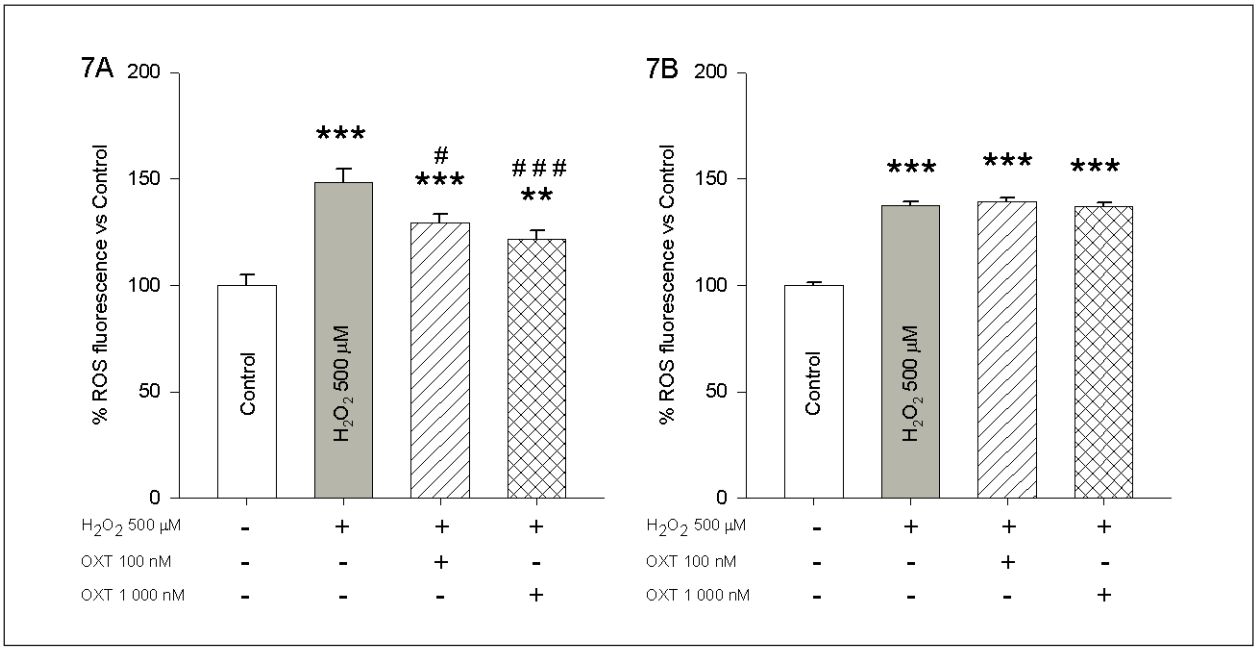

Figure 7. Effects of oxytocin (OXT) on reactive oxygen species (ROS) production induced by H_2O_2. ROS production was measured using H2DCFDA (dichloroflourescin diacetate) kit. Cells were treated for 4 h with 500 µM H_2O_2 in the presence or absence of OXT (100 and 1000 nM). Results are expressed as the mean percentage change of ROS florescence signal compared with untreated controls ± SEM (n=6). Statistical comparisons were performed employing Bonferroni's adjustment for Two-Way ANOVA. Significantly different values are marked with **p<0.01 and ***p<0.001 compared to the control group. #p<0.05 and ###p<0.001 compared to the group treated with 500 µM H_2O_2 alone.

as astroglial and nerve cells, and in hippocampal tissue as well (Havranek et al. 2017; Lin et al. 2017; Palanisamy et al. 2018). OXT was also reported to exert mitogenic actions (Ohmichi et al. 1995; Molnar et al. 1999; Szeto et al. 2017), to regulate cell cycle and neurogenesis (Jafarzadeh et al. 2014; Havranek et al. 2017) and to induce elongation and projection of cells improving neural differentiation (Lin et al. 2017; Lestanova et al. 2017; Zatkova et al. 2018).

In addition to preventing the cell-growth stimulating effects of OXT, cells with OXTR knockdown exhibited a slower rate of growth than that observed for the control U-87MG cells. Similar lower rates in cell proliferation were also observed during treatment with an OXTR antagonist. These findings suggest that either lack of OXTR activation and/or a reduced number of OXTR may negatively affect glial cell growth. It is feasible that those astrocyte-like cells may produce OXT, which through activation of OXTR sustains cell growth and viability. The viability of OXTR knockdown cells is indeed greatly affected. Additionally, OXTR may be an integral part of a pathway needed to sustain cell growth. Suppression of proliferation of the control U-87MG cells and those with OXTR knockdown remains controversial. Possible explanation for these results could be supported by an important role of oxytocin in the regulation of cell cycle (Jafarzadeh et al. 2014; Havranek et al. 2017). Nevertheless, precise function of oxytocin receptors in cell-division cycle should be further investigated. Signal crosstalk between G protein-coupled receptors and/or growth factors needed for normal cell growth, may occur, and if so, account for the slower growth rate observed in the OXTR knockdown cells and in U-87MG cells exposed to an OXTR antagonist (Song and Albers 2018).

In this study, we demonstrated that OXT stimulates ERK1/2 phosphorylation and that this effect seems to be responsible for the growth-stimulating actions of OXT. In fact, inhibition of ERK1/2 with its selective inhibitor PD098059, inhibited cell growth and blocked OXT-induced cell proliferation. Similarly, the stimulating effects of OXT on cell growth and ERK1/2 phosphorylation were inhibited when the U-87MG cells were treated with an OXTR antagonist and in U-87MG KD cells, likewise. These findings further support the role of the MAPK cascade on cell proliferation and survival via OXTR coupled to Gαq protein (Sun et al. 2015), and correspond with studies proving that OXT stimulates ERK1/2 signaling pathway in other experimental models including human embryonic kidney and rat hypothalamic H32 cell lines (Rimoldi et al. 2003; Devost et al. 2008; Cargnello and Roux 2011). Nevertheless, we need to make careful conclusions as oxytocin receptor blockage with consequences on ERK1/2 phosphorylation is most likely not a simple competitive antagonism for a single active site on a receptor. To our knowledge, this is the first study to show that OXT mediates its proliferative effect via activation of MAPK-ERK1/2 signaling pathway in this astrocyte-like cell line.

In further support of our theory that OXT acting on OXTR regulates cell survival, we demonstrated that OXT protects against cell death induced by H_2O_2 and CPT, two pro-apoptotic agents and prevents peroxide-induced ROS production. The observation that OXT's protective effects were not observed in OXTR knockdown cells suggests that OXT acts on OXTR to induce its cell protective actions against consequences of oxidative stress. This is the first study demonstrating that activation of OXTR by OXT inhibits ROS production (basal and stimulated) in astrocyte-like cells. Recently, OXT has been shown to inhibit H_2O_2-induced oxidative damage in peripheral blood lymphocytes (Stanic et al. 2016). Several mechanisms have been proposed to explain the protective effect of oxytocin. In rats, OXT protects against oxidative stress by increasing glutathione levels and decreasing lipid peroxidation and inflammation (Erkanli et al. 2013; Yuan et al. 2016). However, the mechanism, by which oxytocin protects against apoptosis and oxidative stress in brain cells remains to be explored.

As discussed above, the stimulating action of OXT on cell proliferation observed in U-87MG cells was not observed in OXTR knockdown cells. Paradoxically, OXT inhibited (instead of stimulating) cell proliferation in the knockdown cells. It could be proposed that in the absence of functional OXTR, OXT could be acting at a different receptor (i.e. arginine-vasopressin receptors) to inhibit cell proliferation. In fact, OXT and vasopressin can have distinct or even opposing actions and can activate each other's canonical receptors (Song and Albers 2018). Activation of cyclin-dependent kinase inhibitor (p21) and/or of Protein Kinase A, due to OXTR or vasopressin receptor coupling with Gαi and Gαs, respectively, may exert anti-proliferative actions. However, predominant OXTR coupling with Gαq, leading to stimulation of the ERK pathway, may override the cell growth-inhibitory pathway (Lerman et al. 2018). Further, the membrane localization of OXTR may also play a role. For example, OXTR increases cell proliferation when the OXTR are located in the caveolin-rich lipid rafts of the plasma membrane; yet it

inhibits cell proliferation when the OXTR are located out of the caveolin-rich lipid rafts (Gimpl and Fahrenholz 2001; Rimoldi et al. 2003; Herbert et al. 2007; Strunecka et al. 2009). Further research is needed to clarify the mechanism of OXT-induced inhibition of cell growth in the absence of OXTR.

In summary, the development of an OXTR knockdown cell line allowed to characterize the role of OXTR in OXT's actions on cell growth and survival. The present study supports the role of OXT and OXTR on glioblastoma cell proliferation, protection against pro-apoptotic agents and oxidative stress, and inhibition of ROS formation. In addition, this is the first study to show that OXT mediates its proliferative effect via activation of MAPK-ERK1/2 signaling pathway in astrocyte-like cells. OXT may play a role in cell survival and protection from apoptosis and cell death.

Acknowledgments

This work is supported by The President Faculty Research and Development Grant Nova Southeastern University PFRDG 335410 and PFRDG 336398; and the Slovak Research and Development Agency project APVV-15-205. We would like to thank to Zuzana Bacova, PhD., Beau Freedman, and William Rodriguez for their skilled assistance.

References

Akman T, Akman L, Erbas O, Terek MC, Taskiran D, Ozsaran A. The preventive effect of oxytocin to cisplatin-induced neurotoxicity: an experimental rat model. Biomed Res Int 2015, 167235, 2015.

Bakos J, Strbak V, Ratulovska N, Bacova Z. Effect of oxytocin on neuroblastoma cell viability and growth. Cell Mol Neurobiol 32, 891–896, 2012.

Cargnello M, Roux PP. Activation and function of the MAPKs and their substrates, the MAPK-activated protein kinases. Microbiol Mol Biol Rev 75, 50–83, 2011.

Cassoni P, Sapino A, Stella A, Fortunati N, Bussolati G. Presence and significance of oxytocin receptors in human neuroblastomas and glial tumors. Int J cancer 77, 695–700, 1998.

Cassoni P, Marrocco T, Bussolati B, Allia E, Munaron L, Sapino A, Bussolati G. Oxytocin induces proliferation and migration in immortalized human dermal microvascular endothelial cells and human breast tumor-derived endothelial cells. Mol Cancer Res 4, 351–359, 2006.

Cha JH, Choi YJ, Cha SH, Choi CH, Cho WH. Allicin inhibits cell growth and induces apoptosis in U87MG human glioblastoma cells through an ERK-dependent pathway. Oncol Rep 28, 41–48, 2012.

Devost D, Wrzal P, Zingg HH. Oxytocin receptor signalling. Prog Brain Res 170, 167–176, 2008.

Djuzenova CS, Guttler T, Berger S, Katzer A, Flentje M. Differential response of human glioblastoma cell lines to combined camptothecin and ionizing radiation treatment. Cancer Biol Ther 7, 364–373, 2008.

Erkanli K, Senturk GE, Aydin U, Arbak S, Ercan F, Tuncdemir M, Isiksacan N, Bakir I. Oxytocin protects rat skeletal muscle against ischemia/reperfusion injury. Ann Vasc Surg 27, 662–670, 2013.

Filova B, Reichova A, Zatkova M, Srancikova A, Bukatova S, Bacova Z, Bakos J. Expression of synaptic proteins in the hippocampus is modulated by neonatal oxytocin treatment. Neurosci Lett 725, 134912, 2020.

Gimpl G, Fahrenholz F. The oxytocin receptor system: structure, function, and regulation. Physiol Rev 81, 629–683, 2001.

Havranek T, Lestanova Z, Mravec B, Strbak V, Bakos J, Bacova Z. Oxytocin modulates expression of neuron and glial markers in the rat hippocampus. Folia Biol (Czech Republic) 63, 91–97, 2017.

Herbert Z, Botticher G, Aschoff A, Sendemir E, Zermann DH, Arnold R, Mall G, Jirikowski GF. Changing caveolin-1 and oxytocin receptor distribution in the ageing human prostate. Anat Histol Embryol 36, 361–365, 2007.

Iida M, Sunaga S, Hirota N, Kuribayashi N, Sakagami H, Takeda M, Matsumoto K. Effect of glutathione-modulating compounds on hydrogen-peroxide-induced cytotoxicity in human glioblastoma and glioma cell lines. J Cancer Res Clin Oncol 123, 619–622, 1997.

Jafarzadeh N, Javeri A, Khaleghi M, Taha MF. Oxytocin improves proliferation and neural differentiation of adipose tissue-derived stem cells. Neurosci Lett 564, 105–110, 2014.

Jurek B, Slattery DA, Maloumby R, Hillerer K, Koszinowski S, Neumann ID, van den Burg EH. Differential contribution of hypothalamic MAPK activity to anxiety-like behaviour in virgin and lactating rats. PLoS One 7, e37060, 2012.

Lennicke C, Rahn J, Lichtenfels R, Wessjohann LA, Seliger B. Hydrogen peroxide – production, fate and role in redox signaling of tumor cells. Cell Commun Signal 13, 39, 2015.

Lerman B, Harricharran T, Ogunwobi OO. Oxytocin and cancer: An emerging link. World J Clin Oncol 9, 74–82, 2018.

Lestanova Z, Puerta F, Alanazi M, Bacova Z, Kiss A, Castejon AM, Bakos J. Downregulation of oxytocin receptor decreases the length of projections stimulated by retinoic acid in the U-87MG cells. Neurochem Res 42, 1006–1014, 2017.

Lin YT, Chen CC, Huang CC, Nishimori K, Hsu KS. Oxytocin stimulates hippocampal neurogenesis via oxytocin receptor expressed in CA3 pyramidal neurons. Nat Commun 8, 537, 2017.

Marinova Z, Walitza S, Grunblatt E. Effects of oxytocin and arginine vasopressin on the proliferation and differentiation of a serotonergic cell line. J Neural Transm 125, 103–106, 2018.

Meyer M, Berger I, Winter J, Jurek B. Oxytocin alters the morphology of hypothalamic neurons via the transcription factor myocyte enhancer factor 2A (MEF-2A). Mol Cell Endocrinol 477, 156–162, 2018.

Molnar M, Rigo J, Romero R, Hertelendy F. Oxytocin activates mitogen-activated protein kinase and up-regulates cyclooxygenase-2 and prostaglandin production in human myometrial cells. Am J Obstet Gynecol 181, 42–49, 1999.

Ohmichi M, Koike K, Nohara A, Kanda Y, Sakamoto Y, Zhang ZX, Hirota K, Miyake A. Oxytocin stimulates mitogen-activated protein kinase activity in cultured human puerperal uterine myometrial cells. Endocrinology 136, 2082–2087, 1995.

Palanisamy A, Kannappan R, Xu Z, Martino A, Friese MB, Boyd JD, Crosby G, Culley DJ. Oxytocin alters cell fate selection of rat neural progenitor cells in vitro. PLoS One 13, e0191160, 2018.

Pequeux C, Keegan BP, Hagelstein MT, Geenen V, Legros JJ, North WG. Oxytocin- and vasopressin-induced growth of human small-cell lung cancer is mediated by the mitogen-activated protein kinase pathway. Endocr Relat Cancer 11, 871–885, 2004.

Reversi A, Cassoni P, Chini B. Oxytocin receptor signaling in myoepithelial and cancer cells. J Mammary Gland Biol Neoplasia 10, 221–229, 2005.

Rimoldi V, Reversi A, Taverna E, Rosa P, Francolini M, Cassoni P, Parenti M, Chini B. Oxytocin receptor elicits different EGFR/MAPK activation patterns depending on its localization in caveolin-1 enriched domains. Oncogene 22, 6054–6060, 2003.

Song Z, Albers HE. Cross-talk among oxytocin and arginine-vasopressin receptors: Relevance for basic and clinical studies of the brain and periphery. Front Neuroendocrinol 51, 14–24, 2018.

Stanic D, Plecas-Solarovic B, Petrovic J, Bogavac-Stanojevic N, Sopic M, Kotur-Stevuljevic J, Ignjatovic S, Pesic V. Hydrogen peroxide-induced oxidative damage in peripheral blood lymphocytes from rats chronically treated with corticosterone: The protective effect of oxytocin treatment. Chem Biol Interact 256, 134–141, 2016.

Strunecka A, Hynie S, Klenerova V. Role of oxytocin/oxytocin receptor system in regulation of cell growth and neoplastic processes. Folia Biol (Praha) 55, 159–65, 2009.

Sun Y, Liu WZ, Liu T, Feng X, Yang N, Zhou HF. Signaling pathway of MAPK/ERK in cell proliferation, differentiation, migration, senescence and apoptosis. J Recept Signal Transduct 35, 600–604, 2015.

Szeto A, Sun-Suslow N, Mendez AJ, Hernandez RI, Wagner KV, McCabe PM. Regulation of the macrophage oxytocin receptor in response to inflammation. Am J Physiol Metab 312, E183–E189, 2017.

Yuan L, Liu S, Bai X, Gao Y, Liu G, Wang X, Liu D, Li T, Hao A, Wang Z. Oxytocin inhibits lipopolysaccharide-induced inflammation in microglial cells and attenuates microglial activation in lipopolysaccharide-treated mice. J Neuroinflammation 13, 77, 2016.

Zatkova M, Bacova Z, Puerta F, Lestanova Z, Alanazi M, Kiss A, Reichova A, Castejon AM, Ostatnikova D, Bakos J. Projection length stimulated by oxytocin is modulated by the inhibition of calcium signaling in U-87MG cells. J Neural Transm 125, 1847–1856, 2018.